10882 *Inorg. Chem.* **2010**, *49*, 10882–10893
DOI: 10.1021/ic1012389

Inorganic Chemistry
Article

Binary Boron-Rich Borides of Magnesium: Single-Crystal Investigations and Properties of MgB_7 and the New Boride $Mg_{\sim 5}B_{44}$

Alexis Pediaditakis,[†] Melanie Schroeder,[†] Vanessa Sagawe,[†] Thilo Ludwig,[†] and Harald Hillebrecht[*,†,‡]

[†]*Albert-Ludwigs-Universität Freiburg Institut für Anorganische und Analytische Chemie, Albertstrasse 21, D-79104 Freiburg, Germany, and* [‡]*Freiburger Materialforschungszentrum FMF, Stefan-Maier-Strasse 25, D-79104 Freiburg, Germany*

Received June 21, 2010

Single crystals of dark-red MgB_7 were grown from the elements in a Cu-melt. The crystal structure (Pearson symbol *oI*64; space group *Imma*; a = 10.478(2) Å, b = 5.977(1) Å, c = 8.125(2) Å, 2842 reflns, 48 params, $R_1(F)$ = 0.018, $R_2(I)$ = 0.034) consists of a hexagonal-primitive packing of B_{12}-icosahedra and B_2-units in trigonal-prismatic voids. According to the UV−vis spectra and band structure calculations MgB_7 is semiconducting with an optical gap of 1.9 eV. The long B−B distance of 2.278 Å within the B_2-unit can be seen as a weak bonding interaction. The new $Mg_{\sim 5}B_{44}$ occurs beside the well-known MgB_{12} as a byproduct. Small fragments of the black crystals are dark-yellow and transparent. The crystal structure (Pearson symbol *tP*196, space group $P4_12_12$, a = 10.380(2) Å, c = 14.391(3) Å, 4080 reflns, 251 params, $R_1(F)$ = 0.025, $R_2(I)$ = 0.037) is closely related to tetragonal boron-II (*t*-B_{192}). It consists of B_{12}-icosahedra and B_{19+1}-units. With a charge of −6 for the B_{19+1}-units and a Mg-content of ∼20 Mg-atoms per unit cell the observed Mg content in $Mg_{\sim 5}B_{44}$ is quite close to the expected value derived from simple electron counting rules. All compositions were confirmed by EDXS. The microhardness was measured on single crystals for MgB_7 (H_V = 2125, H_K = 2004) and MgB_{12} (H_V = 2360, H_K = 2459).

1. Introduction

Investigations on binary borides of magnesium have rapidly increased during the last years for several reasons. Probably the most important was the unexpected discovery of the superconductivity of MgB_2 in 2001[1] with a T_C of 39 K. Furthermore it was supposed by theoretical calculations[2] that boron-rich borides are promising candidates for high-T_C superconductivity because of the high density of states below the Fermi level which results from the icosahedral units.

In general boron rich borides have interesting material properties like high hardness, high melting points, and great chemical stability.[3] So they may be useful as HT-materials. In case of Mg-borides, they may be used as a part of lightweight composite materials with Mg or Mg-based alloys. Recently further interest came from the expectation of promising HT thermoelectric properties of boron-rich borides like MgB_4,[4] boron carbide,[5] and rare earth borides.[6]

For a deeper understanding of structure−properties relationship, the understanding of the bonding situation is essential.[7] Our recent investigations on ternary boron-rich borides, that is, boridecarbides and boridesilicides, have shown the strong tendency to form compounds that are electron-precise in a way that they fit to the simple electron counting rules of Wade[8] and Longuet-Higgins.[9] This results in semiconducting compounds with band gaps between 2 and 3 eV. Therefore, single crystals are transparent and less or more colorless. Typical examples are *o*-$MgB_{12}C_2$,[10] $Li_2B_{12}C_2$, $LiB_{13}C_2$,[11]

*To whom correspondence should be addressed. E-mail: harald.hillebrecht@ac.uni-freiburg.de. Phone: 0049-761-203 6131. Fax: 0049-761-203 6102.

(1) Nagamatsu, J.; Nakagawa, N.; Muranaka, T.; Zenitani, Y.; Akimitsu, J. *Nature* **2001**, *40*, 63–64.
(2) Soga, K.; Oguri, A.; Araake, S.; Kimura, K.; Terauchi, M.; Fujiwara, A. *J. Solid State Chem.* **2004**, *177*, 498–506.
(3) (a) Telle, R. *Chem. Unserer Zeit* **1988**, *22*, 93–99. (b) Riedel, R. *Adv. Mater.* **1994**, *4*, 549–560. (c) Riedel, R., Ed. *Handbook of Ceramic Hard Materials*; Wiley-VCH: Weinheim, Germany, 2000.
(4) Takeda, M.; Saito, H. Poster presentation PT-163, 28th International conference on Thermoelectrics ICT/ECT July 26−30 **2009**, Freiburg, Germany.
(5) (a) Emin, D. *Phys. Today* **1987**, *20*, 55. (b) Wood, C. *Rep. Prog. Phys.* **1988**, *51*, 459. (c) Samara, G. A.; Tardy, H. L.; Venturini, E.; Aselage, T. L.; Emin, D. *Phys. Rev. B* **1993**, *48*, 1468. (d) Emin, D. *J. Solid State Chem.* **2004**, *177*, 1619–1623.
(6) Mori, T. In *Handbook on the Physics and Chemistry of Rare Earths, Vol 38*; Gschneidner, K. A., Bunzli, J. C., Pecharsky, V., Ed.; Elsevier: Amsterdam, 2008; p 106−173.
(7) Albert, B.; Hillebrecht, H. *Angew. Chem.* **2009**, *121*, 8794–8824. *Angew. Chem., Int. Ed.* **2009**, *48*, 8640−8668.
(8) (a) Lipscomb, W. N. *Adv. Inorg. Chem. Radiochem.* **1950**, *1*, 117. (b) Wade, K. *Adv. Inorg. Chem. Radiochem.* **1976**, *18*, 1.
(9) Longuet-Higgins, H. C.; Roberts, M. d. V. *Proc. Roy. Soc. A* **1955**, *230*, 110.
(10) Adasch, V.; Hess, K.-U.; Ludwig, T.; Vojteer, N.; Hillebrecht, H. *Chem.—Eur. J.* **2007**, *13*, 3450–3458.
(11) Vojteer, N.; Hillebrecht, H. *Angew. Chem.* **2006**, *118*, 172–175. *Angew. Chem., Int. Ed.* **2006**, *45*, 165−168.

Published on Web 11/02/2010

$Mg_3B_{50}C_8$,[12] (colorless), $MgB_{12}Si_2$,[13] and $Li_2B_{12}Si_2$[14] (yellow). Their crystal structures are based on a covalent framework of icosahedra connected by exohedral 2e−2c bonds. Additional small units (C_2, BC_2, Si) in between complete the framework of 2e−2c bonds.

The situation for binary borides is slightly different because the covalent framework must be built up only by boron.[15] For the higher borides (i.e., M/B > 10), it was known that their crystal structures contain condensed icosahedra besides singular B_{12}-icosahedra. Here starts another challenge of the structure chemistry of boron-rich borides. While the electron count of the singular icosahedra seems to be quite clear (B_{12}^{2-}), there are questions for condensed units. This becomes obvious in a special way when existence, stability, crystal structure, and bonding of tetragonal boron II (t-B_{192}) are discussed. This polymorph of boron was obtained by Ploog and Amberger with a CVD-process from BBr_3/H_2 on a hot Ta-filament at 1200°C.[16] The quality of the single crystals was limited so the refinement resulted in an ambiguous structure model.[17] The existence of B_{12}-icosahedra, dimers of face-sharing icosahedra and interstitial B-atoms is clear, but the points, which are important for the electron count, that is, the completeness of the dimers and the site occupation factors of the interstitial B-atoms, were not. This is even more a challenge as t-B_{192} is discussed as a thermodynamically stable form of boron at HP/HT-conditions.[18] Detailed theoretical calculations are done without a clear proof of its structure.[19]

One way to approach to the problem is to investigate binary boron-rich borides with a similar covalent network of boron polyhedra and where the intersticial boron atoms are substituted by cations. With Mg_5B_{44}, we have synthesized and characterized a new binary magnesium boride that can serve as a model structure of t-B_{192}.

A deficit of the boron sites would lead to a different electron count because of the low electron number of boron the detection of an underoccupied boron site is very difficult by powder methods. Furthermore, there are several examples of boron-rich borides known where small amounts of carbon are incorporated into the covalent framework (for example $B_4C/B_{13}C_2$).[7] Finally many boron-rich borides are characterized by a partial occupation of the metal sites. Therefore, X-ray investigations on high quality single crystals followed by a detailed elemental analysis of the crystals under investigation are essential for reliable results.

The binary system Al/B[20] is well-described by the work of Matkovich[15,21] and Higashi.[22] Besides the simple AlB_2, there is a binary variant of β-rhombohedral boron ($AlB_{\sim 31}$[23]) and two forms of AlB_{12}, that is, tetragonal α-AlB_{12}[24] and orthorhombic γ-AlB_{12}.[25] β-AlB_{12}[20] turned out to be a ternary compound with a composition $Al_{2.7}B_{48}C_2$. The knowledge of the system Mg/B is more limited.[20] The existence of the already mentioned hexagonal MgB_2 is clear (AlB_2-type). Single crystals of MgB_4 were grown from a Na-flux and its crystal structure refined.[26] The same group reported on MgB_7 and refined a structure model from powder data.[27] A binary compound with a structure similar to $AlB_{\sim 31}$ and β-rhombohedral boron was reported by several groups,[28−30] but there were still questions on composition and structural details.

Synthesis and crystal growth of boron-rich borides of Mg can be done in an excess of liquid Mg or from eutectic mixtures of Cu/Mg. The application of the second method resulted in the first single crystals of Mg-containing β-rhombohedral boron (i.e., $MgB_{\sim 17}$)[28] and a new orthorhombic compound with a composition $MgB_{\sim 12}$.[31] The crystal structure of the latter is closely related to tetragonal α-AlB_{12} and orthorhombic γ-AlB_{12} with B_{12}-icosahedra and B_{19+1}-units. In contrast to the Al-compounds $MgB_{\sim 12}$ contains a unique B_{20+1}-unit. This explains the different electron need of the framework of boron polyhedral, i.e. B_{12} icosahedra and B_{19+1}-units or B_{20+1}-units, respectively.

In this contribution we report on the new binary boride $Mg_{\sim 5}B_{44}$ and the single-crystal growth of MgB_7, and we discuss the bonding situation.

2. Experimental Section

2.1. Synthesis. 2.1.1. MgB_7. Single crystals of MgB_7 were synthesized from the elements in a Cu/Mg melt. Copper powder (Merck, 99.7%), magnesium turnings (Riedel-de Haën, 99.5%) and boron (ABCR, 99.5%) were mixed in a molar ratio of 300/100/75 (total mass ∼1 g), put into a BN-crucible (diameter 12 mm. height 20 mm) and placed into a Ta ampule (diameter 15 mm, height ∼4 cm) which was sealed by electric arc welding. The reaction mixture was heated in a high temperature furnace (Thermal Technologies Inc.) under Ar atmosphere up to 1600 °C, held for 40 h, cooled with 10 K/h to 800 °C and then cooled down to room temperature with 100 K/h. The melt regulus was treated with nitric acid (Merck, 65%) to remove Cu. The insolvable residue was filtrated. Dark red to black single crystals of MgB_7 were obtained (Figure 1a). MgB_{12}[31] can be synthesized under very similar conditions. A differentiation between single crystals of MgB_7 and MgB_{12} is simple because of the highly diverse appearance of the black MgB_{12} crystals with a bluish shine (Figure 1b). All crystals were stable to air, moisture and oxidizing agents (concentrated HNO_3).

2.1.2. Mg_5B_{44}. Black single crystals of Mg_5B_{44} of irregular shape with a slight yellow transmission in thin areas (Figure 1c and 1d)

(12) Adasch, V.; Schroeder, M.; Kotzott, D.; Ludwig, T.; Vojteer, N.; Hillebrecht, H. *J. Am. Chem. Soc.* **2010**, *132*, 13723–13732.
(13) Ludwig, T.; Hillebrecht, H. *J. Solid State Chem.* **2006**, *179*, 1622–1628.
(14) Vojteer, N.; Schroeder, M.; Röhr, C.; Hillebrecht, H. *Chem.—Eur. J.* **2008**, *14*, 7331–7342.
(15) Matkovich, V. I. *Boron and Refractory Borides*; Springer-Verlag: Berlin, 1977.
(16) Amberger, E.; Ploog, K. *J. Less-Common Met.* **1968**, *15*, 240–241. Amberger, E.; Ploog, K. *J. Less-Common Met.* **1971**, *23*, 21–31.
(17) Vlasse, M.; Naslain, R.; Kasper, J. S.; Ploog, K. *J. Solid State Chem.* **1979**, *28*, 289–301.
(18) Ma, Y.; Prewitt, C. T.; Zou, G.; Mao, H.-K.; Hemley, R. J. *Phys. Rev. B* **2003**, *67*, 174116.
(19) Hayami, W.; Otani, S. *J. Phys. Chem. C* **2007**, *111*, 688–692.
(20) Villars, P.; Calvert, D. *Pearson's Handbook, Crystallographic Data for Intermetallic Phases*; ASM International: Materials Park, OH, 1997.
(21) Matkovich, V. I.; Economy, J.; Giese, R. F. *J. Am. Chem. Soc.* **1964**, *86*, 2337.
(22) Higashi, I. *J. Solid State Chem.* **2000**, *154*, 168–176.
(23) Higashi, I.; Iwasaki, H.; Ito, T.; Lundström, T.; Okada, S.; Tergenius, L. E. *J. Solid State Chem.* **1989**, *82*, 230–238.
(24) Higashi, I.; Sakurai, T.; Atoda, T. *J. Solid State Chem.* **1977**, *20*, 67–77.
(25) Higashi, I. *J. Solid State Chem.* **1983**, *47*, 333–349.
(26) Naslain, R.; Guette, A.; Barret, M. *J. Solid State Chem.* **1973**, *8*, 68–85.
(27) Guette, A.; Barret, M.; Naslain, R.; Hagenmuller, P. *J. Less-Common Met.* **1981**, *82*, 325–334.
(28) Adasch, V.; Hess, K.-U.; Ludwig, T.; Vojteer, N.; Hillebrecht, H. *J. Solid State Chem.* **2006**, *179*, 2900–2907.
(29) (a) Brutti, S.; Colapietro, M.; Calducci, G.; Barba, L.; Manfrinetti, P.; Palenzona, A. *Intermetallics* **2002**, *10*, 811–817. (b) Giunchi, G.; Malpezzi, L.; Masciocchi, N. *Solid State Sci.* **2006**, *6*, 1202–1206.
(30) Hyodo, H.; Araake, S.; Hodoi, S.; Soga, K.; Sato, Y.; Terauchi, M.; Kimura, K. *Phys. Rev. B* **2008**, *77*, 024515.
(31) Adasch, V.; Hess, K.-U.; Ludwig, T.; Vojteer, N.; Hillebrecht, H. *J. Solid State Chem.* **2006**, *179*, 2916–2926.

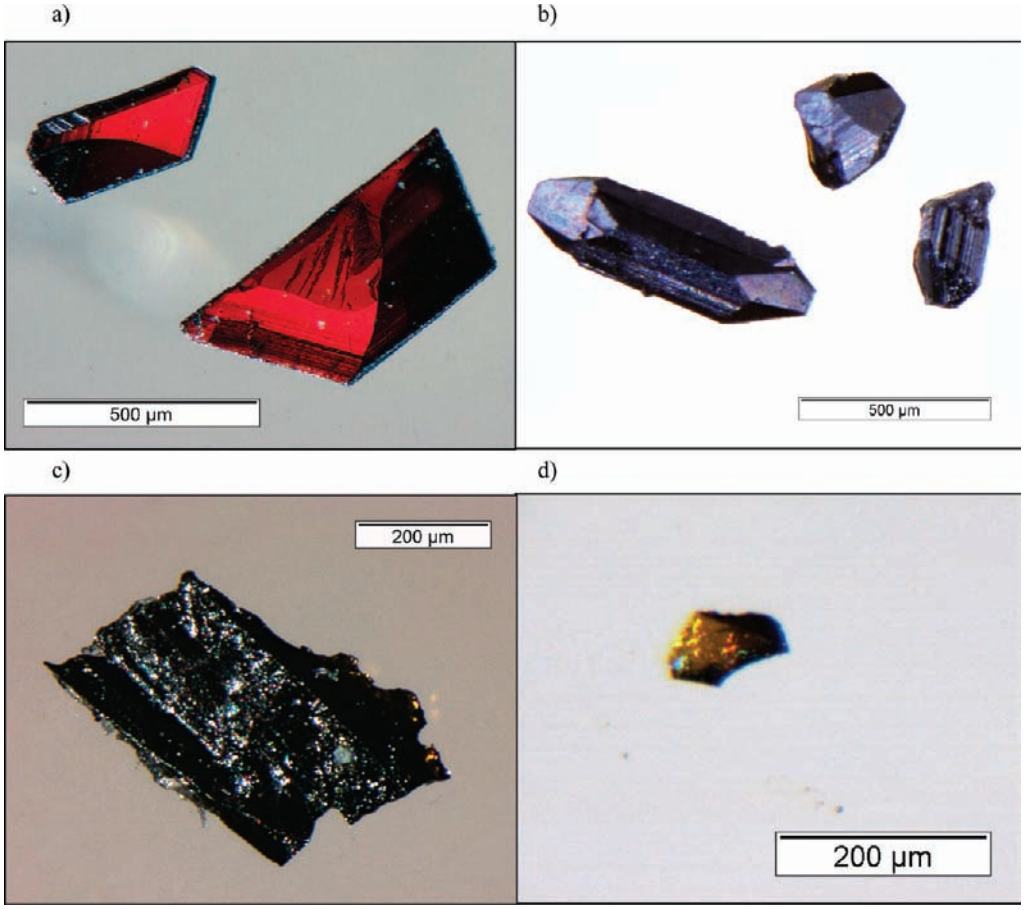

Figure 1. Crystals of Mg/B: (a) red MgB_7, (b) bluish-black MgB_{12}, (c) irregular Mg_5B_{44}, and (d) thin yellow platelet of Mg_5B_{44}.

were casually yielded as a byproduct of the synthesis of MgB_7 and MgB_{12}.

The XRD of a powdered sample showed the reflections of MgB_7 and MgB_{12}. Reflections of Mg_5B_{44} which were calculated from the single crystal data could not be observed.

2.2. Elementary Analysis. Qualitative and quantitative analyses of single crystals of MgB_7, Mg_5B_{44} and MgB_{12} were performed by EDXS measurements. These investigations took place on a scanning electron microscope Zeiss DSM 962 with EDX-unit Oxford Inca 300. The samples were fixed with electrical conducting glue on a graphite platelet mounted on an aluminum sample holder. Embedding and polishing was not performed because of the excellent surfaces of the single crystals which allowed good results.

All EDXS measurements are in very good agreement with the composition determined by X-ray diffraction. In all cases, only boron and magnesium as the only elements with $Z > 4$ were confirmed. Especially for carbon this is not trivial as carbon is frequently present in commercial boron samples or may result from other contaminations and small amounts can contribute significantly to structure and stability of boron-rich borides ($Mg_2B_{24}C$,[32] $Al_{2.7}B_{48}C_2$[33]). According to the experience with other boron-rich borides and boridecarbides the possible carbon content is below 5−10%, the reliability is ±1 atom % for Mg and ±2 atom % for B. As shown in Table 1, the decreasing Mg content in the row MgB_7−Mg_5B_{44}−MgB_{12} could be validated.

2.3. Structure Solution and Refinement. 2.3.1. MgB_7. The X-ray single crystal data were collected on an Enraf-Nonius CAD 4 automatic 4-circle diffractometer with graphite monochromated MoKα radiation. Because of the low absorption coefficient of $\mu = 0.33$ mm^{-1}, no absorption correction was applied. The indexing routine resulted in a bodycenterd orthorhombic unit cell. Lattice parameters of $a = 10.478(2)$ Å, $b = 5.977(1)$ Å, and $c = 8.125(2)$ Å were obtained from 25 high angle reflections. According to the additional reflection condition $hk0$ for reflections with $h = 2n$ space group *Imma* (No. 74) was assumed. The refinement was started with the existing structure model derived from powder data.[27] Its refinement converged at R values of $R_1(F) = 0.018$ and $R_2(I) = 0.042$. All boron atoms were refined with anisotropic displacement parameters and showed small and almost uniform displacements. The two magnesium positions show full occupation with different displacement parameters according to the different surroundings (see below). The deficit of the Mg-sites (95% occupation) reported by Guette et al. was not confirmed. Compared to the structure refinement in ref 27, a significant enhancement of the quality of the structure solution was attained by using high-angle single crystal data.

Table 1. Composition of Selected Boron-Rich Magnesium Borides, Errors for EDXS Measurement: ±1 atom % for Mg, ±2 atom % for B

	Mg (at. %)		B (at. %)		Mg/B ratio	
	X-ray	EDXS	X-ray	EDXS	X-ray	EDXS
MgB_7	12.5[a]	13.1	87.5[a]	86.9	1:7	1:6.6
Mg_5B_{44}	9.7(1)[b]	10.5	90.3	89.6	1:9.3	1:8.5
MgB_{12}	7.5(2)[b]	7.9	92.5	92.1	1:12.3	1:11.6

[a] Assumed as stoichiometric (see text). [b] Standard deviation for Mg from refinement.

(32) Adasch, V.; Hess, K.-U.; Ludwig, T.; Vojteer, N.; Hillebrecht, H. *J. Solid State Chem.* **2006**, *179*, 2150–2157.
(33) Meyer, D. PhD Thesis, University Freiburg, Germany, 1999.

Table 2. Details of the Crystal Structure Determination of MgB_7

composition in unit cell	Mg_8B_{56}
Z	8
molar weight	99.98 g mol^{-1}
crystal shape and color	flat rod, dark red, transparent
crystal dimensions	0.1 × 0.2 × 0.4 mm
crystal system	orthorhombic
space group	*Imma* (No. 74)
lattice parameters	a = 10.4782(16) Å, b = 5.9769(9) Å, c = 8.1245(19) Å
cell volume	508.81 Å^3
calculated density	2.610 g cm^{-3}
temperature of measurement	294 K
range (*hkl*)	$0 \le h \le 28$, $-16 \le k \le 16$, $-22 \le l \le 22$
range (2Θ)	0−150°
radiation	Mo Kα, graphite monochromator
diffractometer	Nonius CAD4
scan modus/measurement	Ω/2Θ-scan, 0.70° + 0.40 tan Θ 120 s
reflections measured	11 509
unique reflections	2842 (2193 with $I > 2\sigma(I)$)
number of parameters	48
absorption coefficient	0.33 mm^{-1}
extinction[35]	0.019(3)
residual electron density	+0.63 e/Å^3, −0.38 e/Å^3, σ = 0.08 e/Å^3
weighting function[35]	0.0211/0.0
internal R-value	R_{int} = 0.029 (R_s = 0.022)
GOF	1.007
R-values	$R_1(F > 4\sigma(F_o))$ = 0.018, $R_1(F)$ = 0.034, $R_2(I)$ = 0.042

Table 3. Atomic Coordinates, Fractional Occupation Factors (f.o.f.), and Displacement Parameters U_{eq}/Å^2 for MgB_7 (esd's in Parentheses)

atom	site	x	y	z	f.o.f.	U_{eq}
Mg1	4*a*	0.5	0	0.5	0.994(1)[a]	0.00505(2)
Mg2	4*e*	0.5	0.75	0.88429(2)	0.998(1)[a]	0.01661(4)
B1	8*i*	0.33263(2)	0.25	0.57392(2)	0.998(2)[a]	0.00386(2)
B2	8*i*	0.58356(2)	0.75	0.22494(2)	0.999(2)[a]	0.00399(2)
B3	16*j*	0.68650(1)	0.59402(2)	0.08644(2)	1	0.00401(2)
B4	16*j*	0.82803(1)	0.00276(2)	0.70540(2)	1	0.00393(2)
B5	8*i*	0.39129	0.25	0.36547(2)	1.004(2)[a]	0.00423(2)

[a] Complete occupation assumed.

Different single crystals were measured for structure refinement. Details for the best refinement of a single crystal are summarized in Table 2. Atom coordinates, displacement parameters and fractional occupation factors are shown in Table 3, the anisotropic displacement parameters are given in the supplemental data. Selected distances are listed in Table 4. Further details on the structure refinement (complete list of distances and angles) may be obtained from Fachinformationszentrum Karlsruhe, D-76344 Eggenstein-Leopoldshafen, Germany, fax: +49 724 808666, e-mail: crysdata@fiz-karlsruhe.de) on quoting the registry number CSD-421896.

Brown-transparent single crystals of MgB_7, which were obtained as a byproduct from the synthesis of *o*-$MgB_{12}C_2$,[34] showed a significant deficit on the Mg sites (Mg1: 80.0%, Mg2: 87.4%). A similar variation of color is observed for $Mg_xB_{50}C_8$ ($2.4 < x < 4$).[12]

2.3.2. Mg_5B_{44}. Investigations of a Mg_5B_{44} single crystal were performed with a single crystal-diffractometer with curved image plate detector (R-AXIS Spider, Rigaku Inc.), Mo Kα radiation,

(34) Schroeder, M. PhD Thesis, University Freiburg, Germany, 2009.
(35) Sheldrick, G. M. *SHELXL*; University of Göttingen: Göttingen, Germany, 1997.

Table 4. Selected Distances in MgB_7 in Å (esd's in Parentheses)

endohedral B−B distances, Ø = 1.823 Å					
B3−B4[b]	1.7834(4)	B2−B3[b]	1.8162(3)	B3−B4[b]	1.8523(3)
B4−B4[a]	1.7887(4)	B1−B4[b]	1.8240(3)	B2−B1[a]	1.8552(4)
B1−B3[a]	1.7956(3)	B2−B4[b]	1.8336(3)	B3−B3[a]	1.8645(4)
exohedral B−B distances, Ø = 1.774 Å					
B4−B5[b]	1.7473(3)	B2−B2[a]	1.7511(5)	B3−B3[b]	1.7989(4)
B1−B5[a]	1.8016(5)	B5···B5	2.2781(5)		
Mg−B distances					
Mg1−B5[b]	2.1737(3)			Mg2−B5[a]	2.3271(5)
Mg1−B1[b]	2.3809(3)			Mg2−B3[b]	2.7176(4)
Mg1−B4[b]	2.4560(4)			Mg2−B4[b]	2.7643(3)
Mg1−B2[b]	2.8272(4)			Mg2−B3[b]	2.8466(3)
				Mg2−B2[a]	2.9028(4)

[a] Distances occur two times. [b] Distances occur four times.

and graphite monochromator. They revealed a tetragonal unit cell with the lattice parameters a = 10.380(2) Å and c = 14.391(3) Å. Although symmetry and dimension suggested an analogy to α-AlB_{12}[24] a new ab initio structure solution with direct methods (SHELXTL[35]) was performed. Because of the low absorption coefficient (μ = 0.29 mm^{-1}), no correction of absorption effects was necessary. The Laue-class 4/*mmm* and serial reflection conditions l = 4 for reflections 00*l* and h = 2 for reflections *h*00, lead to the possible space groups $P4_12_12$ (No. 92) and $P4_32_12$ (No. 96). A structure model was obtained with direct methods. Because of the low anomalous dispersion of this light-atom structure, a determination of the absolute structure is difficult and structural models for both space groups were refined. During the structure refinement, it became obvious that slightly better R-values could be obtained in space group $P4_12_12$.

The refinement converged at R values of R_1 = 0.025 and R_2 = 0.064 on basis of a data set of 4080 independent reflections ($2\Theta_{max}$ = 75°) and 251 free variables. The unit cell contains 4 formula units. 176 boron atoms on 21 fully occupied general positions and two special positions could be identified. All boron atoms have been refined with anisotropic displacement parameters and showed, as expected, small and almost isotropic displacement with only small variations. The values are comparable to those in MgB_7 and other boron-rich borides. The refined occupation factors are very close to the ideal values with only small standard deviations, which indicate a complete occupation by boron. The magnesium atoms are distributed over five partially occupied sites with occupation factors from 43 to 54%. Mg1/Mg2 and Mg3 show extended displacement ellipsoids, which are caused by the surroundings in the boron framework. Diffuse scattering caused by the disordered Mg-atoms was clearly seen on the image plate pictures. The sum of occupation factors leads to the composition $Mg_{19.1(1)}B_{176}$ or $Mg_{4.75}B_{44}$, respectively. With respect to the problem of Mg-disorder this is in good agreement with the composition obtained by EDXS investigations leading to the composition $Mg_{20.7}B_{176}$. For simplification, this new compound will be named as Mg_5B_{44} in this publication.

Several single crystals from different batches were measured for structure refinement. Details for the best refinement are summarized in Table 5. The atom coordinates, displacement parameters and fractional occupation factors are shown in Table 6. The anisotropic thermal displacement parameters are in the Supporting Information. Selected distances are given in Table 7. Further details on the structure refinement (complete list of distances and angles) may be obtained from Fachinformationszentrum Karlsruhe, D-76344 Eggenstein-Leopoldshafen, Germany, fax: +49 724 808666, e-mail: crysdata@fiz-karlsruhe.de) on quoting the registry number CSD-421897.

Table 5. Details of the Crystal Structure Determination of Mg_5B_{44}

composition in unit cell	$Mg_{19}B_{176}$
Z	4
molar weight	597.2 g mol^{-1}
crystal shape and color	irregular fragment, dark metallic
crystal dimensions	0.25 × 0.2 × 0.1 mm
crystal system	tetragonal
space group	$P4_12_12$ (No. 92)
lattice parameters	a = 10.3795(15)Å, c = 14.391(3)Å
cell volume	1550.40 Å^3
calculated density	2.558 g/cm^3
temperature of measurement	294 K
range (hkl)	$-17 \le h \le 16$, $-17 \le k \le 17$, $-24 \le l \le 24$
range (2Θ)	0−75°
radiation	Mo Kα, graphite monochromator
diffractometer	Rigaku R-Axis SPIDER
scan modus/measurement	120 frames with 4.5 min w = 48°, c = 54°, f = 0°, Dw = 1.2° 100 frames with 4.5 min w = 50°, c = 54°, f = 180°, Dw = 1.2°
reflections measured	37 948
unique reflections	4080 (3933 with $I > 2\sigma(I)$)
number of parameters	251
absorption coefficient	0.29 mm^{-1}
extinction[35]	0.000(3)
Flack parameter	0.03(9)
residual electron density	+0.37 e Å^{-3}, −0.30 e Å^{-3}, σ = 0.06 e Å^{-3}
weighting function[35]	0.0294/0.35
internal R-value	R_{int} = 0.034 (R_s = 0.021)
GOF	1.143
R values	$R_1(F > 4s(F_o))$ = 0.025, $R_1(F)$ = 0.037, $R_2(I)$ = 0.064

2.4. UV−vis spectra. The single-crystal UV−vis spectra were measured in transmission at room temperature with a JASCO V-570 UV−vis/NIR photometer in a range from 200 to 2500 nm.

2.5. Calculations. For the calculations, the FP-LAPW (full potential linearized augmented plane wave) method was used. The exchange and correlation were treated within the GGA (generalized gradient approximation) using the Engel−Vosko version with the WIEN2k-program package.[36] For the calculations the following muffin-tin radii R_{mt} were used: Mg = 2.04 au (105.1 pm), B = 1.64 au (87 pm). Self-consistency was achieved by demanding that convergence of the total energy to be smaller than 10^{-5} Ry/cell and a charge distance about 10^{-5}. The cutoff-energy was $R_{mt} \cdot k_{max}$ = 6.5. The integration of Brillouin zone to determine total and partial DOS (TDOS, PDOS) was carried out by the tetrahedron method (500 k-points/BZ; 64/IBZ). A 7 × 7 × 7 Monkhorst-Pack-Grid was used. Beyond that the standard settings of Wien2k (version 09.2) were used. Effective charges of Mg were derived according to the Bader-method as implemented in Wien2k (J.O. Soto, G.N. Garcia in[36]). Valence charge distribution (ρ_{val}) was described with the program xcrysden.[37]

2.6. Microhardness Measurements. Microhardness was measured with a microhardness equipment MHT 10 (producer: A. Paar, Austria). A force of 2 N generated within 10 s and applied for 15 s. The imprints of the indenters (Vickers hardness, square pyramid; Knoop, rhombic pyramid) were evaluated and converted into a value for the microhardness according to the usual procedures.[38]

(36) Blaha, P., Schwarz, K., Madsen, G. K. H., Kvasnicka, D., Luitz, J. *WIEN2K-An Augmented Plane Wave and Local Orbital Program for Calculating Crystal Properties*, version 09.2; TU Wien: Vienna, Austria, 2001.
(37) Kokalj, A. *J. Mol. Graph. Mod.* **1999**, *17*, 176.
(38) DIN EN 6507.

Table 6. Atomic Coordinates, the Fractional Occupation Factors (f.o.f.), and Displacement Parameters U_{eq}/Å^2 for Mg_5B_{44} (esd's in Parentheses)

atom	Wyckoff	x	y	z	f.o.f.	U_{eq}
Mg1	8b	0.19783(5)	0.12524(5)	0.23383(4)	0.535(2)	0.0094(1)
Mg2	8b	0.42009(5)	0.48367(5)	0.18132(4)	0.533(2)	0.0074(1)
Mg3	8b	0.16425(11)	0.10132(8)	0.16457(6)	0.440(2)	0.0237(3)
Mg4	8b	0.43763(6)	0.11721(6)	0.15043(4)	0.441(2)	0.0049(2)
Mg5	8b	0.20982(6)	0.01519(6)	0.37486(4)	0.438(2)	0.0054(2)
B1	8b	0.12803(7)	0.23996(8)	0.37611(6)	1	0.0055(1)
B2	8b	0.04009(8)	0.13894(8)	0.45861(5)	1	0.0055(1)
B3	8b	0.04790(7)	0.31226(8)	0.47695(5)	1	0.0057(1)
B4	8b	0.04159(8)	0.39119(8)	0.36463(5)	1	0.0055(1)
B5	8b	0.01893(7)	0.11067(8)	0.32979(5)	1	0.0055(1)
B6	8b	0.03125(7)	0.27161(8)	0.27735(5)	1	0.0052(1)
B7	8b	0.38867(8)	0.27610(8)	0.25712(5)	1	0.0055(1)
B8	8b	0.39891(8)	0.11336(8)	0.31063(5)	1	0.0061(1)
B9	8b	0.37753(7)	0.39456(8)	0.34592(5)	1	0.0053(1)
B10	8b	0.37899(7)	0.30929(8)	0.45548(5)	1	0.0050(1)
B11	8b	0.38764(8)	0.14250(8)	0.43847(5)	1	0.0055(1)
B12	8b	0.29414(7)	0.24133(7)	0.36234(5)	1	0.0050(1)
B13	8b	0.18422(8)	0.43914(7)	0.13732(5)	1	0.0056(1)
B14	8b	0.10981(8)	0.29639(7)	0.17261(5)	1	0.0057(1)
B15	8b	0.28882(7)	0.30130(8)	0.15430(5)	1	0.0057(1)
B16	8b	0.03047(8)	0.38196(8)	0.08642(5)	1	0.0054(1)
B17	8b	0.03498(8)	0.21024(8)	0.07616(5)	1	0.0064(1)
B18	8b	0.30926(8)	0.40145(8)	0.04996(5)	1	0.0059(1)
B19	8b	0.31281(8)	0.22621(7)	0.04543(5)	1	0.0055(1)
B20	8b	0.14869(8)	0.45432(8)	0.00655(5)	1	0.0060(1)
B21	8b	0.30696(8)	0.05658(7)	0.02533(5)	1	0.0059(1)
B22	4a	0.16509(8)	0.16509(8)	0	1	0.0059(2)
B23	4a	0.46004(8)	0.46004(8)	0	1	0.0059(2)

3. Results and Discussion

3.1. Crystal Structure of MgB_7. Our results confirm and specify the findings of Guette et al..[27] The crystal structure of MgB_7 (Figure 2) consists of B_{12}-icosahedra, B_2-units, and Mg^{2+} cations. The icosahedra form a hexagonal-primitive packing with the B_2 units and Mg2 filling trigonal-prismatic voids. Mg1 is located in the center of the rectangular plane between two B_2 units. The B_{12} icosahedra are quite regular with endohedral distances between 1.783 and 1.864 Å (Ø = 1.823 Å). The layers of icosahedra are formed by four longer exohedral bonds (1.799 Å) and orientated perpendicular to the a-axis. This explains the pseudohexagonal metric and its significant deviation from the ideal value ($c/b = 1.39 < \sqrt{3}$). The layers are linked in direction [100] by two shorter exohedral bonds (1.751 Å). Alternatively, the packing of the icosahedra can also be described as a hexagonal rod packing. The exohedral connections of the icosahedra are completed by six bonds to the B_2-units (1.747−1.802 Å). Vice versa, each B-atom of the B_2-unit (B5) has three bonds to the icosahedra. All these distances are in the range of the sum of the single bond radii (0.88 Å) and represent "normal" 2e−2c bonds. The tetrahedral surrounding of B5 is completed by a fourth distance of 2.278 Å (Figure 3a). According to Pauling's approximation,[39] this distance corresponds to a bond order of 0.2. A quantification of the different surroundings is possible with the bond-valence method of O'Keeffe.[40] For the B-atoms of the icosahedron the bond orders to other boron atoms, that is, within the covalent framework, sum up to bond orders of 3.1 to 3.2. For B5 this value is 2.0. A comparable value for B5 is obtained if the short

(39) Pauling, L. *Die Natur der Chemischen Bindung*; VCH-Verlag: Weinheim, Germany, 1964.
(40) O'Keeffe, M.; Brese, N. *J. Am. Chem. Soc.* **1991**, *113*, 3226–3229.

Table 7. Selected Distances in Mg_5B_{44} (in Å) (esd's in Parentheses)

endohedral B−B distances of B_{12} icosahedra, Ø = 1.823 Å					
B5−B10	1.749(1)	B9−B10	1.808(1)	B5−B6	1.838(1)
B10−B11	1.751(1)	B3−B8	1.811(1)	B7−B12	1.840(1)
B10−B12	1.752(1)	B3−B4	1.813(1)	B7−B8	1.860(1)
B4−B6	1.769(1)	B1−B4	1.816(1)	B8−B11	1.868(1)
B1−B6	1.771(1)	B5−B9	1.817(1)	B2−B7	1.868(1)
B7−B9	1.777(1)	B2−B3	1.820(1)	B8−B12	1.871(1)
B11−B12	1.787(1)	B9−B12	1.826(1)	B1−B5	1.878(1)
B6−B11	1.805(1)	B1−B2	1.828(1)	B2−B5	1.890(1)
B4−B11	1.805(1)	B4−B8	1.831(1)	B2−B9	1.893(1)
B6−B10	1.806(1)	B1−B3	1.833(1)	B3−B7	1.904(1)
endohedral B−B distances of B_{19+1} unit, Ø = 1.820 Å					
B14−B16[a]	1.734(1)	B16−B21[a]	1.807(1)	B16−B20[a]	1.841(1)
B13−B14[a]	1.746(1)	B13−B15[a]	1.813(1)	B13−B18[a]	1.849(1)
B15−B19[a]	1.767(1)	B18−B19[a]	1.820(1)	B13−B16[a]	1.854(1)
B19−B22[a]	1.784(1)	B19−B19	1.824(2)	B20−B21[a]	1.861(1)
B19−B21[a]	1.785(1)	B14−B17[a]	1.825(1)	B18−B20[a]	1.863(1)
B17−B21[a]	1.787(1)	B18−B23[a]	1.827(1)	B18−B19[a]	1.864(1)
B16−B17[a]	1.789(1)	B19−B20[a]	1.834(1)	B14−B15[a]	1.877(1)
B17−B22[a]	1.8012(9)	B15−B18[a]	1.838(1)	B21−B22[a]	1.8894(9)
exohedral B−B distances of B_{12} icosahedra, Ø = 1.796 Å					
B10−B10	1.640(1)	B9−B17	1.742(1)	B2−B2	1.877(1)
B4−B16	1.699(1)	B11−B3[a]	1.749(1)	B5−B23	1.952(1)
B6−B14	1.733(1)	B7−B15	1.825(1)	B8−B20	1.976(1)
B12−B1[a]	1.736(1)				
exohedral B−B distances of B_{19+1} units, Ø = 1.804 Å					
B16−B4[a]	1.698(1)	B13−B21[b]	1.753(1)	B20−B8[a]	1.976(1)
B14−B6[a]	1.733(1)	B15−B7[a]	1.825(1)		
B17−B9[a]	1.742(1)	B23−B5[a]	1.952(1)		
Mg−B distances > 2.8 Å					
Mg1−B (11×)	2.186(1)−2.480(1)			Mg4−B (12×)	2.199(1)−2.471(1)
Mg2−B (14×)	2.304(1)−2.654(1)			Mg5−B (15×)	2.310(1)−2.786(1)
Mg3−B (11×)	2.107(1)−2.649(2)				
Mg−Mg distances					
Mg1−Mg3	1.089(2)	Mg2−Mg3	2.041(2)	Mg2−Mg2	2.431(1)
Mg1−Mg5	2.336(1)	Mg2−Mg5	2.384(1)	Mg4−Mg5	2.004(1)

[a] Distances occur two times. [b] Distances occur four times.

distance to Mg1 is taken into account because the distance B5−Mg1 2.174 Å corresponds to a bond order of 0.6.

The Mg-atoms are located in quite different voids of the icosahedral framework. Mg2 (Figure 3b) in the trigonal-prismatic void of the icosahedra's packing is coordinated by 14 boron atoms which come from six edges (2.718−2.903 Å) and one B_2-unit, which are the shortest distances (2.327 Å). The average is 2.76 Å. Mg1 (Figure 3c) has a coordination number of 16, that is, 12 B-atoms from 4 icosahedral planes (2.381−2.827 Å) and 4 very short distances to two B_2-units (2.174 Å). Here the average amounts to 2.35 Å. The difference between the two Mg atoms makes an impact on the displacement parameters. The U_{eq}-values are different by a factor of 3. In comparison to other Mg-containing boron-rich boridecarbides ($Mg_2B_{24}C$,[32] $MgB_{12}C_2$,[10] $Mg_xB_{50}C_8$ ($x = 2.4-4.0$)[12]) the value for Mg1 is the smallest ever found and that for Mg2 the largest one. The shape of the displacement ellipsoids is

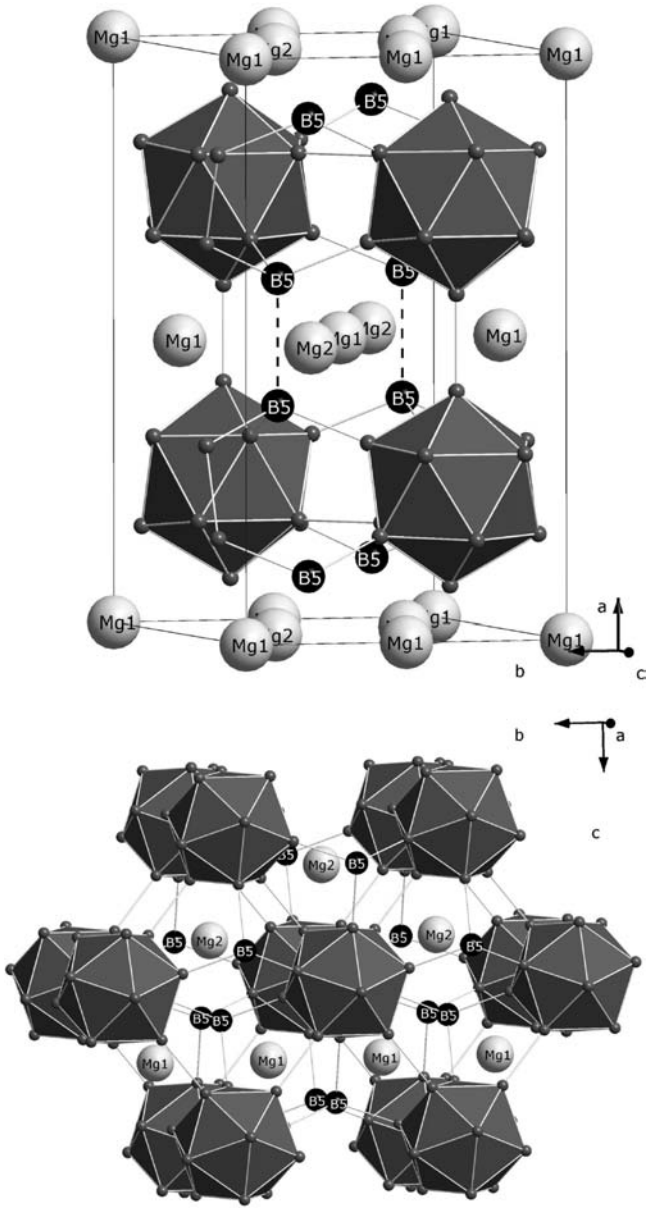

Figure 2. Crystal structure of MgB_7. Top: Unit cell. Bottom: Projection in direction [100].

a result of the geometry of the surrounding. Low-temperature investigations have shown that the anisotropy of Mg 2 is mainly because of thermal movement.[41] A similar behavior was observed for the Li^+ cation in $Li_2B_{12}Si_2$.[14] The clear difference between the two Mg atoms becomes also evident in the calculation of the bond valence. Mg1 has a bond order of 4.5 and Mg2 of 1.6. Calculated bond order and size of displacement parameters agree very well to the findings for MgB_2.[42−44] Here the Mg−B distance of 2.504 Å (BO = 0.25) corresponds to a bond valence sum of 3.0 (CN = 12). Accordingly the displacement parameters

(41) Geis, V. Diploma Thesis, University Freiburg,Germany, 2009.
(42) Mori, H.; Lee, S.; Yamamoto, A.; Jajima, S. *S. Sato Phys. Rev. B* **2002**, *65*, 092507.
(43) Schmidt, J.; Schnelle, W.; Grin, Yu.; Kniep, R. *Solid State Sci.* **2003**, *5*, 535–539.
(44) Tsirelson, V.; Stash, A.; Kohout, M.; Rosner, H.; Mori, H.; Sato, S.; Lee, S.; Yamamoto, A.; Tajima, S.; Grin, Yu. *Acta Crystallogr. B* **2003**, *59*, 575–583.

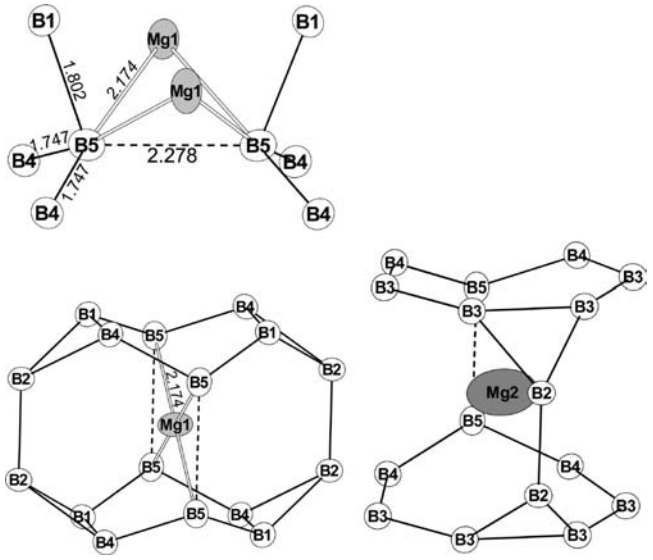

Figure 3. Coordination of B5, Mg1, and Mg2 in MgB_7. Distances in Å. Ellipsoids (!) represent 99% probability.

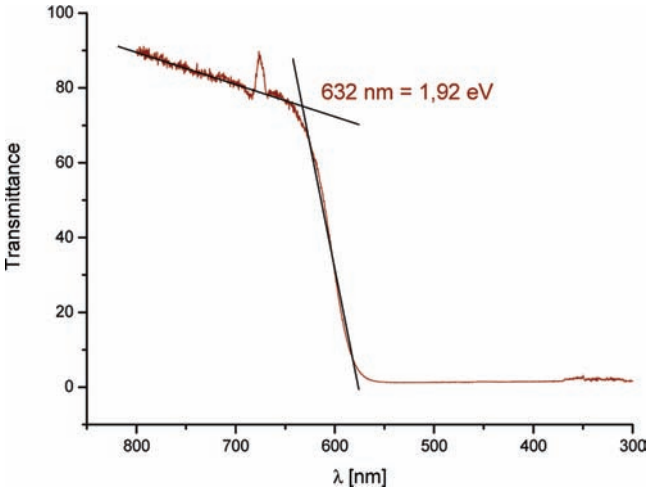

Figure 4. UV−vis spectrum of a MgB_7 single crystal in transmission.

of Mg and B are nearly equal and very similar to Mg1 in MgB_7.

3.1.1. Optical Investigation of MgB_7. The UV−vis spectrum of a MgB_7 single crystal (Figure 4) was measured in transmission. It shows the typical behavior of a semiconductor with an optical band gap. The extrapolation of the onset gives a band gap of 1.92 eV (632 nm). This is in very good agreement with the red color of the crystal. Similar observations were made for yellow $Li_2B_{12}Si_2$ (547 nm, 2.27 eV)[14] yellow $MgB_{12}Si_2$ (540 nm, 2.30 eV)[13,34] and colorless *o*-$MgB_{12}C_2$ (480 nm, 2.58 eV).[41]

3.1.2. Band Structure Calculations on MgB_7. Representations of T-DOS and P-DOS are shown in Figure 5. The T-DOS performs a clear band gap of 1.84 eV, which fits excellent to the optical data. Furthermore, it agrees to the description of MgB_7 as an electron-precise compound. There is a limited mixing of s- and p-states of boron. As expected the states close to the Fermi level are dominated by the boron p-states. According to the crystal structure the boron atoms forming the icosahedron (B1−B4) are very similar but the states of B5 are clearly different. The representation of the

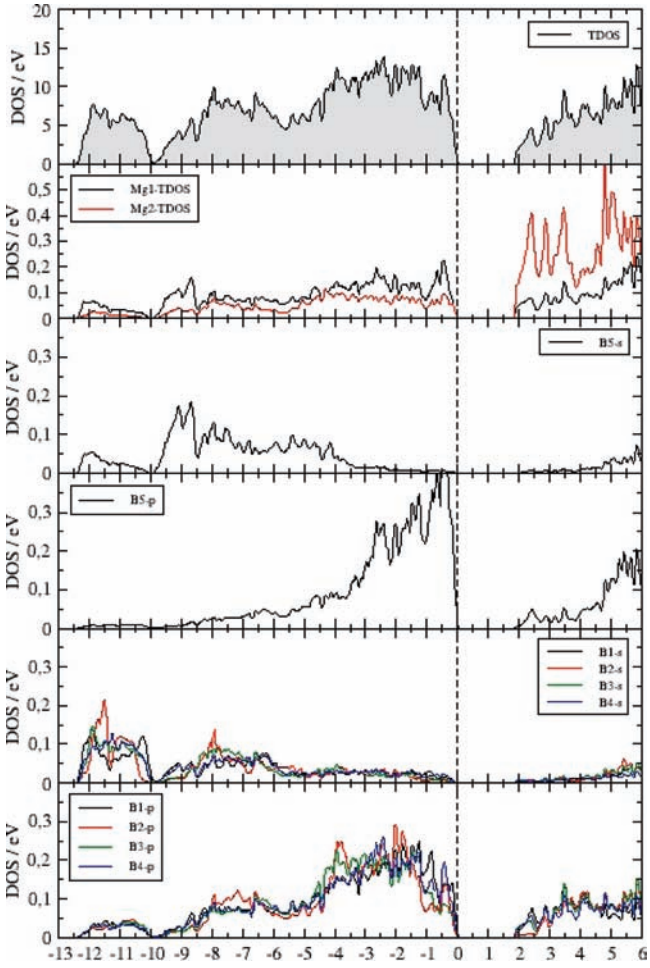

Figure 5. Band structure calculations for MgB_7.

P-DOS for the different B-atoms shows the highest occupied states have a very large share of B5. This correlates to a weak bonding interaction between the B-atoms of the B_2-unit. Similar observations were made for *o*-$MgB_{12}C_2$. This structure is closely related to MgB_7. It shows the same number of electrons. Within the same covalent framework of B_{12}-icosahedra the B_2-units are exchanged by C_2-units with a remarkably long C−C distance of 1.73 Å. Here the states close to the Fermi level are also dominated by the p-states of carbon, but less distinctive than in MgB_7.

The participation of the Mg states is quite small according to the mainly ionic interaction of Mg. Interestingly the contribution of Mg1 is significantly higher than that of Mg2, especially close to the Fermi level around −1 eV. This might be due to the short distances Mg1−B5, which were already discussed. Nevertheless, the calculated electron density shows no distinctive covalent shares (Figure 6).

An important point is the charge transfer from the Mg-atoms to the boron framework and the "ionicity" of MgB_7. The method of Bader allows the determination of effective charges and resulted in values of +1.70 for Mg1 and +1.72 for Mg2. This justifies again the description of MgB_7 as an electron-precise or electronically balanced compound with a nearly complete electron transfer.

The theoretical investigations allow a representation of the calculated electron density. Figure 7 shows a cutout with the different B−B bonds. As expected the highest electron density is found for the short exohedral 2e-2c

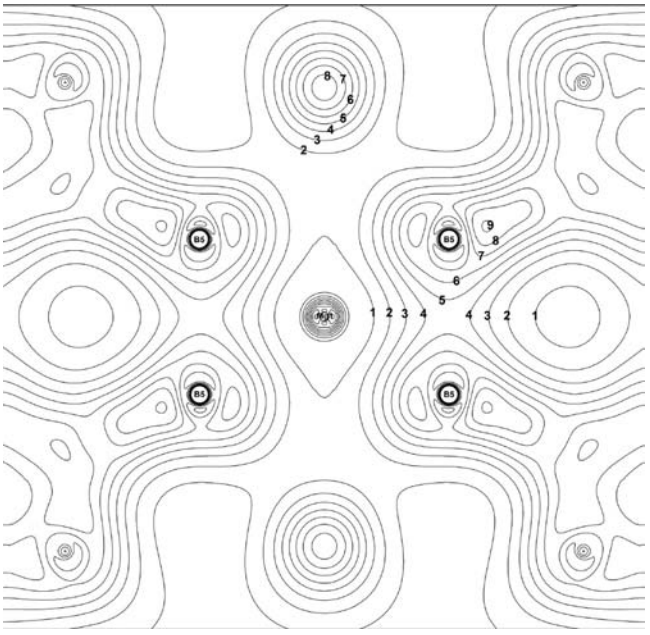

Figure 6. Calculated valence electron density around Mg1 in MgB_7; contour lines correspond to 0.1 $e^-/Å^3$.

bond B2−B2 (1.751 Å). Furthermore the density is slightly reduced for the longer exohedal bonds B1−B5 (1.802 Å). Lower values are observed for the endohedral 2e−3c bonds of the icosahedron (B1−B2 = 1.855 Å). A significant electron density of 0.48 $e^-/Å^3$ is also found between the B5 atoms. This is about half the value of the other B−B bonds. In each case the topological analysis of the electron density reveals clearly a bond critical point between the boron atoms. Remarkably this is even true for the long distance B5−B5. Therefore we expect also from the calculated electron density a weak but bonding interaction between the atoms B5 within the B_2-unit.

The charges for Mg in MgB_7 are in a remarkable agreement to the findings for MgB_2. Schmidt et al. proposed a nearly complete charge transfer $Mg_{0.98}{}^{2+}(B_2)^{1.5-}(0.46e^-)$ on the base of TB-LMTO-ASA and ELF methods. The same approach explained the significant Al-deficit in isotypic $Al_{0.9}B_2$.[45] The results of Tsirelson et al.[44] who investigated the electron density in MgB_2 by X-ray diffraction and theoretical calculations are in good agreement to our findings. For Mg they calculated a charge of +1.5 (TB-LMTO) and +1.6 (FPLO), respectively, which is slightly larger than that from experimental X-ray data (multipole refinement: charge transfer of 1.4 e^-). Furthermore they point out that the Mg−B interaction is only partially ionic. In general the charge separation Mg ↔ B is smaller in MgB_2 than in MgB_7. This is expected because of the well-developed band gap of MgB_7 and from the high stability of $B_{12}{}^{2-}$ (for example $B_{12}H_{12}{}^{2-}$, $B_{10}C_2H_{12}$). So MgB_7 is in between of MgB_2 (2D metal)[46] and typical ionic Mg-compounds like MgO (+1.85)[47] and Mg_2SiO_4 (+1.79/+1.84).[48]

In general the theoretical and optical investigations justify a simple picture where two electrons were transferred to the icosahedron and two to the B_2-unit. The formal description of MgB_7 as $(Mg^{2+})_2(B_{12})^{2-}(B_2)^{2-}$ is supported by a comparison to other boron-rich borides which are closely related to MgB_7. They have the same arrangement of icosahedra but different intericosahedral units of two or three atoms and therefore different electron needs and different metal contents. *o*-$MgB_{12}C_2$ with a C_2 unit was already mentioned.[10] Further examples are the colorless compounds $LiB_{13}C_2$ with a CBC unit $[(Li^+(B_{12})^{2-}(CBC)^+]$[11] and $LiB_{12}PC$ with a disordered PC unit $[Li^+(B_{12})^{2-}(PC)^+]$.[49] The similar $ScB_{13}C$ contains a disordered BC unit.[50] Furthermore there is a long row of ternary borides with a composition $MAlB_{14}$ (M = Li, Na, Mg, Y, rare earth metal) where the occupation of the metal sites is in a way that (nearly) four electrons are supplied for the boron framework and Al is on site 4*d*. Examples are $LiAlB_{14}$[51] $NaAlB_{14}$,[52] $Mg_{0.79}Al_{0.80}B_{14}$,[53] $Y_{0.62}Al_{0.71}B_{14}$,[54] and $Dy_{0.63}Al_{0.74}B_{14}$.[55]

3.1.3. Microhardness Measurements. Boron-rich borides are of interest as hard materials.[3] The formation of well-shaped MgB_7 and MgB_{12} single crystals enabled the determination of the microhardness. Because the values of the microhardness are influenced by the way of measurement (crystal size, crystal preparation, force and time of force application, etc.) we have measured additionally the hardness of α-AlB_{12} under the same conditions on crystals of similar size. Microhardness values for MgB_7 according to the method of Vickers are H_V = 2125 (20.4 GPa). The method of Knoop yielded a hardness of H_K = 2004 (= 19.3 GPa). The values for MgB_{12} are higher with H_V = 2360 (22.9 GPa) and H_K = 2345 (22.8 GPa). The highest hardness was observed for α-AlB_{12}, that is, H_V = 2445 (23.8 GPa) and H_K = 2459 (23.9 GPa), which are in good agreement with the published values of 23 GPa.[56] The increase of hardness from MgB_7 to MgB_{12} can be explained by an enlarged share of covalent bonding (B_{19+1} instead of B_2 with the long B−B distance). The increase from MgB_{12} to α-AlB_{12} fits to the observation that substitution by a cation with a higher charge enlarges the (micro)hardness due to stronger ionic interaction and shorter distances (Mg > Li[12]).

3.2. Crystal Structure of Mg_5B_{44}. The boron framework of Mg_5B_{44} is isotypic to α-AlB_{12} and consists of B_{12} icosahedra and B_{19+1} units (Figure 8). The B_{12} icosahedra are generated by 12 crystallographic different boron atoms (B1−B12). Each icosahedron is connected by two opposing boron atoms to two other icosahedra forming a rod of icosahedra. These rods are packed to layers and the

(45) Burkhardt, U.; Gurin, V.; Haarmann, F.; Borrmann, H.; Schnelle, W.; Yaresko, A.; Grin, Yu. *J. Solid State Chem.* **2004**, *177*, 389–394.
(46) Kortus, J.; Mazin, I. I.; Belashchenko, K. D.; Antropov, V. P.; Boyer, L. L. *Phys. Rev. Lett.* **2001**, *86*, 4656.
(47) Sasaki, S.; Fujino, K.; Takeuchi, Y. *Proc. Japan Acad. B* **1079**, *55*, 43–48.
(48) Sasaki, S.; Fujjino, K.; Takeuchi, K.; Sadanaga, R. *Acta Crystsllogr. A* **1980**, *36*, 904–915.
(49) (a) Vojteer, N. Stauffer, J.; Neikom, C. Barros, V.; Hillebrecht, H. 16th International Symposium on Boron, Borides and Related Materials ISBB2008, 7.-12.9.2008, Matsue, Japan. (b) Vojteer, N. Stauffer, J.; Schroeder, M. Hillebrecht H. *Chem—Eur. J.* In press
(50) (a) Shi, Y.; Leithe-Jasper, A.; Tanaka, T. *J. Solid State Chem.* **1999**, *148*, 250–259. (b) Leithe-Jassper, A.; Sato, A.; Tanaka, T. *Z. Kristallogr. NCS* **2003**, *216*, 45.
(51) Ito, T.; Higashi, I. *Acta Crystallogr. B* **1983**, *39*, 239–243.
(52) Okada, S.; Tanaka, T.; Sato, A.; Shishido, T.; Kukou, K.; Nakajima, K.; Lundström, T. *J. Alloys Compd.* **2005**, *395*, 231–235.
(53) Higashi, I.; Ito, T. *J. Less-Common Met.* **1983**, *92*, 239–246.
(54) Kursukova, M. M.; Lundström, T.; Tergenius, L. E.; Gurin, V. N. *J. Alloys Compd.* **1992**, *187*, 39–48.
(55) Derkhachenko, L. I.; Gurin, V. N.; Korzukova, M. M.; Nechitailov, A. A.; Nechitailov, A. P.; Kuzma, Y. B.; Chaban, N. F. *AIP Conf. Proc* **1991**, *231*, 451–455.
(56) Gurin, V.; Derkachenko, L. I. *Proc. Crystal Growth Charact.* **1993**, *27*, 163–199.

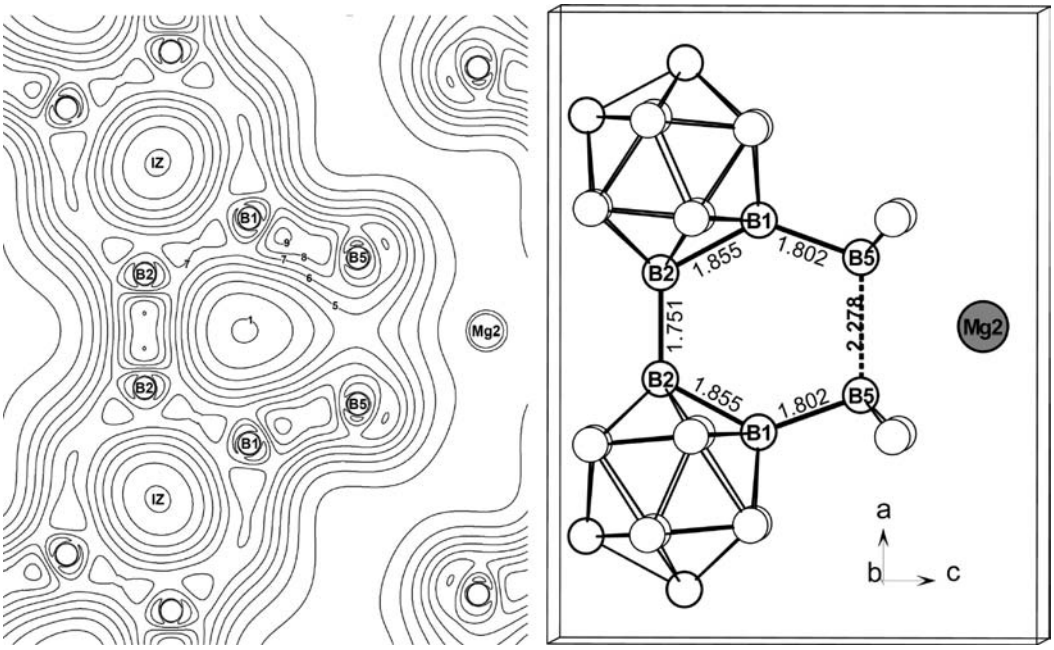

Figure 7. Calculated valence electron density of the B_2-unit in MgB_7 with the corresponding cutout of the crystal structure; contour lines correspond to 0.1 $e^-/Å^3$; atoms with rims in bold are in the drawing plane.

layers are stacked in direction [001] with alternating orthogonal orientation of the rods. This type of a tetragonal rod packing[57] builds a three-dimensional network of rods of icosahedra parallel to the *a*-axes, intersecting the (100) plane in *x* 1/4 3/8 and *x* 3/4 7/8 and a second type of rods parallel to the *b*-axis crossing the (010) plane in 1/4 *y* 5/8 and 3/4 *y* 1/8. The basic structure of icosahedra creates helical gaps between the rods which are occupied by B_{19}-units. The B_{19}-unit consists of ten crystallographic inequivalent boron atoms (B13−B22) and can be described as a twinned icosahedron with two vacant site, that is, two boron atoms are missing from a *closo*-structure. Every B_{19}-unit has an additional single boron atom (B23), which caps the vertex B18−B18. It connects the B_{19}-unit to two icosahedra, belonging to different orthogonal rods. The B_{19}-unit including the single boron atom will be named as B_{19+1}-unit in this work. The B_{19+1}-unit has C_2 symmetry, the 2-fold symmetry axis runs through B22 and B23 (Figure 9, top). This unit is already known from the compounds α-AlB_{12}[24] and γ-AlB_{12}.[25] Many boron-rich borides contain very similar condensed units, which are figured by condensed icosahedra, for example, the B_{19+1}-unit with C_s-symmetry in γ-AlB_{12}[25] and the B_{20+1} unit in MgB_{12}[31] (Figure 9, bottom). In addition, the polymorphs of elemental boron contain related units like the B_{21+1} unit in β-tetragonal boron II (*t*-B_{192})[17] and the B_{27}/B_{28} unit in β-rhombohedral boron.[20,58]

The B_{12} icosahedra are fairly regular. Every boron atom has five endohedral bonds and one exohedral bond. The exohedral bonds are connected to other B_{12} icosahedra or a B_{19+1}- unit. The intraicosahedral bond lengths range from 1.751 Å to 1.907 Å (average 1.823 Å) in high accordance with other boron-rich borides. While intraicosahedral bonds are usually considered as 2e−3c bonds, exohedral bonds are expected to be 2e−2c bonds. In fact,

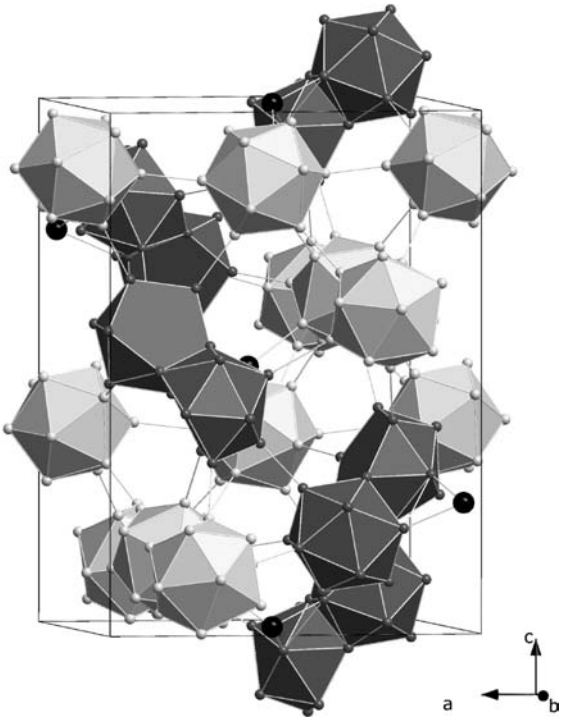

Figure 8. Boron framework of Mg_5B_{44} (light gray, B_{12} icosahedra; dark gray, B_{19+1} unit; black, single boron atom B23).

there is only little information available on the electronic situation in boron-rich borides. The application of theoretical methods is difficult because of the complexity of structures, their large unit cells, partial occupations and disordered atoms. However in these complex crystal structures a tendency to shorter B−B distances in exohedral, and longer distances in endohedral bonds is visible. In Mg_5B_{44} the exohedral bond lengths are shorter on average (1.796 Å) and vary in a greater interval from 1.644 to 1.979 Å.

(57) O'Keeffe, M.; Anderson, S. *Acta Crystallogr. A* **1977**, *33*, 914–923.
(58) Slack, G. A.; Hejna, C. I.; Garbauskas, M. F.; Kasper, J. S. *J. Solid State Chem.* **1988**, *76*, 52–63.

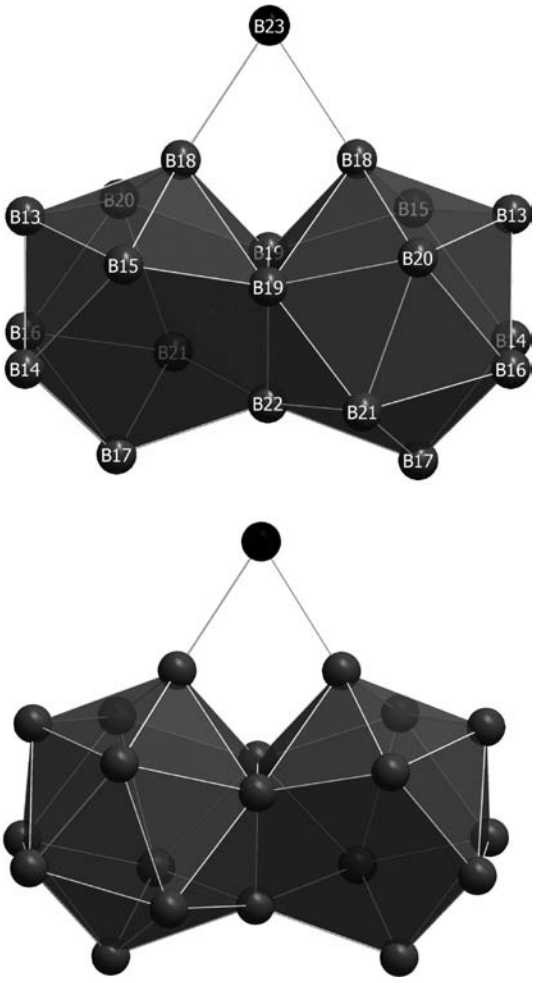

Figure 9. B_{19+1} unit in Mg_5B_{44} (top) and B_{20+1} unit in MgB_{12} (bottom).

The situation in the B_{19+1}-unit is very similar to the icosahedra. The endohedral distances are between 1.737 and 1.924 Å (average: 1.820 Å). The exohedral distances range from 1.698 to 1.976 Å (average 1.804 Å). As well in this case, the exohedral distances vary in a greater interval and seem to be slightly shorter in average than the endohedral distances. No exohedral bonds result for B19 and B22 which connect the two icosahedra. Between the two B18-atoms of the same B_{19+1} unit there is a quite long distance of 1.974 Å. It is not clear, if this distance should be treated as an endo- or exohedral distance. In fact, the real electronic situation of the triangular face which is built by the atoms B18−B18−B23 and the bonding of the isolated B23 (B23−B5 = 1.954 Å, B23−B18 = 1.827 Å) is not clear. On basis of difference Fourier maps, Higashi et al.[59] suggest for α-AlB_{12} a three-center bonding between B18−B18−B23. For Mg_5B_{44} the situation seems to be in between a 2e−2c and a 2e−3c bond (Figure 10).

As usual in boron-rich borides, the metal positions in Mg_5B_{44} are located in the interstitial voids of the framework of boron polyhedra. In comparison to the ionic radii of the metal, these interstitial spaces are quite large. A contraction or expansion of the rigid, covalent boron framework is only possible to a lower extend. Because of the larger ionic radius of magnesium (0.86 Å) compared to aluminum (0.67 Å)[60] and the higher metal content, an expansion of the crystal structure should be observed. Actually, only a small increase of the unit cell dimensions of Mg_5B_{44} (a = 10.380(2) Å and c = 14.391(3) Å) can be observed in comparison to α-AlB_{12} (a = 10.158(2) Å and c = 14.270(5) Å).[24]

All Mg−B distances are in a range which is known from other Mg-borides (i.e., > 2.11 Å). The size of the framework-forming units (B_{12}, B_{19+1}) results in large and asymmetric voids. Therefore the coordination numbers of the metal atoms are high and the coordination spheres irregular. This might be responsible for the frequently observed behavior of boron-rich borides with disorder of the metal sites. In α-AlB_{12} the interstitial space neighboring the pentagonal face of the B_{19+1}-unit is occupied by a disordered Al-atom, which is described by three split positions with very different occupation factors (Al1: 72%, Al3: 24%, Al5: 2%).[24,59] In Mg_5B_{44}, the same void is occupied by Mg3, which is directly neighbored by two other Mg positions Mg1/Mg2 (Figure 11). These three Mg positions show a partial occupation, which is associated with very short Mg−Mg distances (Mg1−Mg3 = 1.09 Å, Mg2−Mg3 = 2.04 Å). The site occupation factors sum up in a way that the occurrence of unrealistically short distances (i.e. < 2.3 Å) is avoided. All of these Mg sites, in particular the Mg3 position, exhibit enlarged displacement parameters, pointing to a tendency of disorder. A description with split positions was not possible in the refinement. The Mg5 position corresponds to the Al4 position in α-AlB_{12} (occupation 15%) with a Mg5−Mg4 distance around 2.00 Å (Figure 11). This distance is also too short for a simultaneous occupation, which is expressed in partial occupation factors around 45−50%. Both site occupation factors sum up to a nearly complete occupation (88%). The shortest Mg−Mg distances between Mg-atoms of different voids are between 2.3 and 2.4 Å. For Mg4 and Al2 (occupation 49%) there exist no corresponding sites.

In comparison to α-AlB_{12}, the sum of the Mg occupation factors in Mg_5B_{44} is higher, but the resulting electron transfer from the metal atoms to the boron framework is nearly the same. The Mg occupation factors are very similar and close to 0.5, which is in contrast to α-AlB_{12} (Al1 75%, Al4 16%).[59] The partial occupation of the Mg-sites results in diffuse scattering which was clearly detected in the course of the single crystal investigations. The diffuse streaks did not show any signs of ordering. The disorder of Mg and especially of Mg3 is nearly independent from temperature. A measurement at 120 K revealed slightly reduced displacement parameters, in contrast to MgB_7. Therefore we assume a static disorder. Only one of the sites Mg4/Mg5 is occupied. For Mg1/Mg2/Mg3, the situation is more complex. In sum, two of the three sites are occupied. Because Mg3 is between Mg1 and Mg2 there is a strong but not unique correlation. This might explain the displacement parameters of Mg3. Despite the different surroundings for all Mg-sites the effective coordination numbers are very similar. The calculation of bond orders according to O'Keeffe allows a qualitative estimation and gives comparable values between 4.15 and 4.19 with Mg4 as an exception (5.13).

For the discussion on site occupation factors and displacement parameters it should be mentioned that both are biased and standard deviations do not represent an error. This is important for the comparison of results of X-ray investigations and EDXS.

(59) Ito, T.; Higash, I.; Sakurai, T. *J. Solid State Chem.* **1979**, *28*, 171–184.
(60) Shannon, R. D.; Prewitt, C. T. *Acta Crystallogr. B* **1969**, *25*, 925.

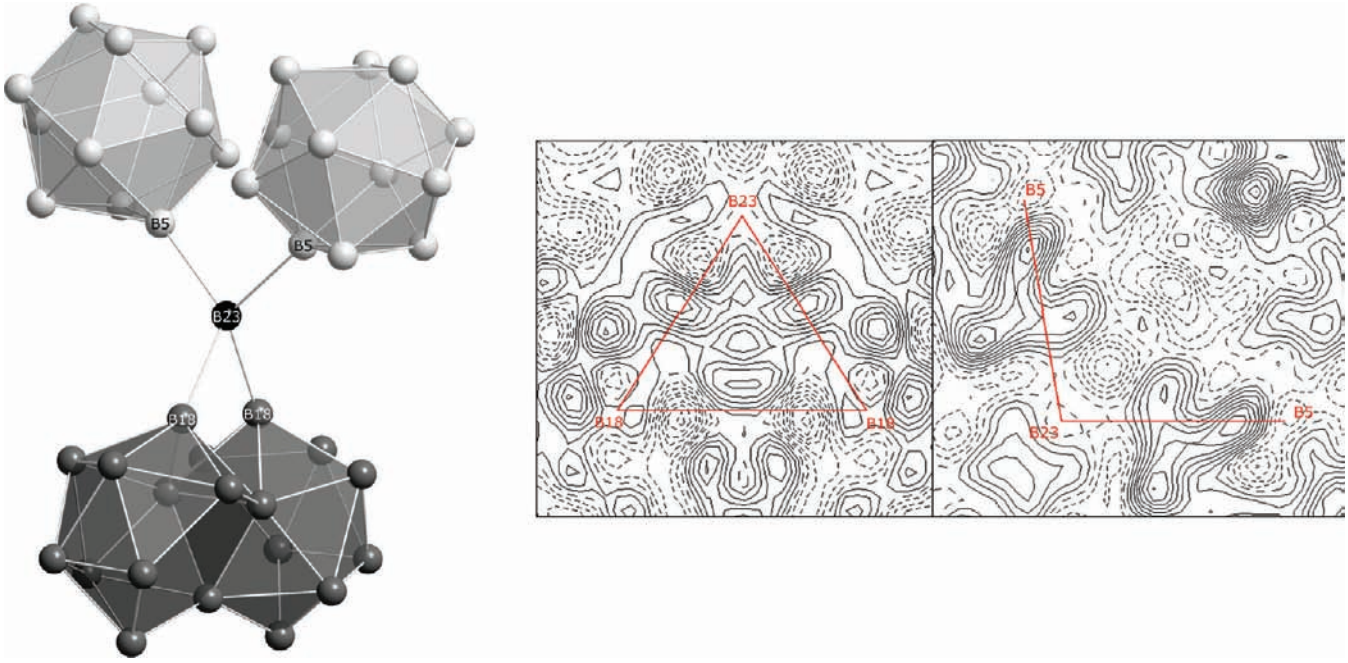

Figure 10. Surrounding of B23 (left) and difference Fourier maps (right) of the exohedral bonds B23−B18, B18−B18 (left), and B23−B5(right).

In boron-rich solids containing complex boron polyhedra the question arises, which electronic demand can be dedicated to the different forms of these polyhedra for stability. For the B_{12} icosahedron with 12 exohedral 2e−2c bonds, the rules of Wade[8] and Longuet-Higgins[9] predict a demand of 2 additional electrons. This statement is well affirmed by the charge donation of the metals in numerous borides.[7] The determination of electronic requirements of more complex polyhedra, like the B_{19+1}-unit, is more difficult. With the *mnopq*-rule of Jemmis et al.[61] a further development of the rules of Wade for more complex polyhedra has been given. By the term $m + n + o + p - q$ (m = number of condensed polyhedra, n = number of skeletal atoms, o = number of single atom bridges between polyhedra, p = number of missing atoms from being *closo*-structure and q = number of atoms overcapping a triangular face of the cluster), the number of bonding MOs in this cluster can be calculated. The suitability of the *mnopq*-rule to boron clusters in boron-rich solids was confirmed.[62] The application of this rule to the B_{19+1}-unit gives $m=2, n=20, o=1, p=2, q=0$, leading to a skeletal electronic demand of 25 electron pairs or 50 electrons, respectively. Twenty boron atoms supply 60 electrons, of which 16 electrons are needed for 16 exohedral 2e−2c bonds, leading to a difference of 6 electrons. The same value was stated for α-AlB_{12} by Higashi on the basis of deformation electron density studies and theoretical calculations.[59] This charge has to be supported from the metal ions. In the boron framework of α-AlB_{12} and Mg_5B_{44}, there are 4 B_{19+1} units, furthermore 8 B_{12} icosahedra per unit cell, leading to an electronic requirement of 40 electrons. By addition of the occupation factors of the metal positions, in α-AlB_{12} there are 13.0 Al atoms (39.0 electrons), in Mg_5B_{44} 19.1 Mg Atoms (38.2 electrons). The assumption of complete occupations by Mg1/Mg2/Mg3 and Mg4/Mg5 results in 20 Mg atoms per unit cell.

According to the *nmopq*-rule and the electron density studies on α-AlB_{12} both compounds are electron-precise compounds. This is supported for Mg_5B_{44} by the crystal color. Very thin parts of the crystal are dark-yellow in transmission (Figure 1c and d) indicating a band gap around 2.3 eV similar to $Li_2B_{12}Si_2$ and $MgB_{12}Si_2$.

For MgB_{12} with B_{20+1}-units (charge −4) the idealized composition referring to the unit cell size of Mg_5B_{44} and α-AlB_{12} would be $Mg_{16}B_{180}$, i.e. 32 electrons are required for the boron framework according to the *nmopq*-rule. The refinement of the single crystal data revealed a slightly lower Mg-content resulting in 29.2 electrons.[31] The reduced electron need by the substitution of B_{19+1} through B_{20+1} is evident. The larger deviation from the idealized value might explain the bluish-black color of the crystals (Figure 1b).

According to our refinement all boron sites in Mg_5B_{44} are completely occupied. The displacement parameters are very similar in size and remarkably uniform. Due to the limited crystal quality this was not the case for the refinement of the structure of *t*-B_{192}. The displacement factors of boron atoms of the boron polyhedra differ by a factor of 6, those of the intersticial boron atoms even by a factor of 10. This limits significantly the reliability of statements concerning completeness of the boron polyhedra (closo/nido/arachno...) and the extent of electron transfer by the intersticial boron atoms. It is well-known that displacement parameters and occupation factors are coupled, especially for low quality X-ray data. A simulation for our data of Mg_5B_{44} shows, that a difference of displacement parameters as observed for *t*-B_{192} corresponds to changes of the occupation factors by 40−60%. Therefore the discussion of stability and electronic situation in *t*-B_{192} on the basis of the published structure model is somewhat tentative.

(61) Jemmis, E. D.; Balakrishnarajan, M. M.; Pancharatna, P. D. *J. Am. Chem. Soc.* **2001**, *123*, 4313–4323.
(62) Jemmis, E. D; Prasad, D. L. V. K. *J. Solid State Chem.* **2006**, *179*, 796–802.

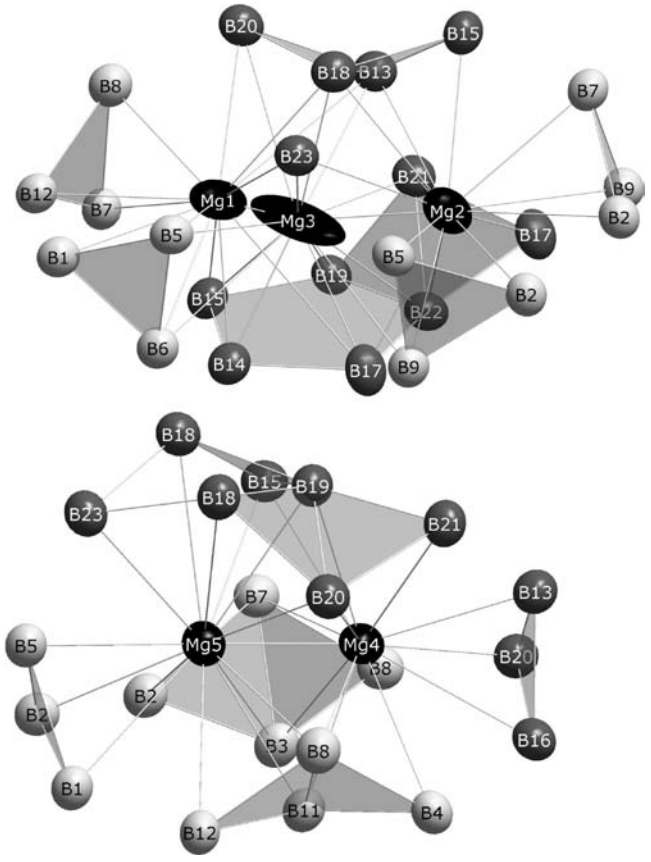

Figure 11. Mg surroundings in Mg_5B_{44}, displacement ellipsoids represent 99% probability, planes of the boron polyhedral are drawn.

4. Conclusions

Our results on MgB_7 confirm the strong tendency of boron-rich borides to realize electron-precise structures. The structure of MgB_7 consists of B_{12}-icosahedra and B_2-units with a remarkably long B−B distance of 2.278 Å. While the stability of the closo-cluster $(B_{12})^{2-}$ is obvious and well-known it is surprising that the long B−B distance contains a bonding interaction. This becomes evident from the dark-red color of the crystals, UV−vis spectra and the results of band structure calculations, which confirm existence and size of the optical band gap (∼1.9 eV). According to the calculated electron density there is a bond critical point between the two B-atoms. The valence electron density is about 50% of a normal covalent B−B bond. This is accompanied by short Mg−B distances. Therefore the formula MgB_7 can be written as $(Mg^{2+})_2(B_{12})^{2-}(B_2)^{2-}$. This is in a line with other boron-rich borides *o*-$MgB_{12}C_2$, $LiB_{13}C_2$, and $LiB_{12}PC$, which are colorless and show the same arrangement of B_{12} icosahedra. Because of the excellent quality of the single crystal X-ray data an experimental determination of the electron density is in preparation. Preliminary results confirm the electron distribution as it was obtained from the band structure calculations.

The structure of the novel binary boride Mg_5B_{44} is closely related to α-AlB_{12}. It consists of B_{12} icosahedra and B_{19+1}-units forming a 3D-framework. Mg is located in two different types of voids with partial occupations close to 50%. Assuming charges of −2 for the B_{12} icosahedra and −6 for the B_{19+1} units, a composition of Mg_5B_{44} results in an electron-precise compound. This is quite close to the findings by means of X-rays ($Mg_{4.75}B_{44}$) and EDXS ($Mg_{5.2}B_{44}$) and is supported by the dark-yellow color of thin crystal fragments.

The *nmopq*-rules of Jemmis can be applied to the boron-rich borides MgB_{12} (or $Mg_{\sim 15}B_{180}$) and Mg_5B_{44}.($Mg_{20}B_{176}$). Structural findings and EDXS measurements confirm the higher electron demand of the B_{19+1} unit of Mg_5B_{44} with two missing B-atoms in the double-icosahedron and a formal charge of −6 compared to the B_{20+1} unit in MgB_{12} with one missing B-atom and an expected charge of −4.

The findings for Mg_5B_{44}, MgB_{12}, and α-AlB_{12} are important for the structure of tetragonal boron II (*t*-B_{192}). A comparison of the structures of β-rhombohedral boron[58] and its binary variants LiB_{10} ($Li_{30}B_{309}$)[63] and $MgB_{\sim 17}$[28] shows that the frameworks of boron polyhedra including the deficit on one boron site are identical and only the interstitial B atoms of β-rh. boron are exchanged by metal cations. For *t*-B_{192} the situation is more complex. The example of Mg_5B_{44} and MgB_{12} shows that different arrangements of the boron polyhedra are possible and stable. The structure model of Ploog et al. stated a complete B_{21+1}-unit for *t*-B_{192}. This represents the most "electron-saving" variant but according to the uncertainties of the refinement its existence is not proven and other polyhedra might be possible.

Concerning possible applications the high chemical and thermal stability of the boron-rich borides MgB_7 and Mg_5B_{44}/MgB_{12} which are electronically balanced and contain icosahedra and condensed moieties should be mentioned.

Acknowledgment. Thanks are due to Dr. Dominik Kotzott for microhardness measurements and to Dipl.-Chem. Stefanie Haseloff for EDXS measurements.

Supporting Information Available: Further data of the structure refinement. This information is available free of charge via the Internet at http://pubs.acs.org.

(63) Vojteer, N.; Stauffer, J.; Hillebrecht, H.; Hofmann, K.; Panda, M.; Albert, B. *Z. Anorg. Allg. Chem.* **2009**, *635*, 653–659.